



Research article

Relationship between the major parameters of warm-blooded organisms' life activity and the properties of aqueous salt solutions

Anatoliy I. Fisenko¹, Oleksii V. Khorolskiy^{2,*}, Nikolay P. Malomuzh³ and Artur A. Guslisty⁴

¹ Oncfec, Inc., 625 Evans Avenue, Suite 1108, Toronto, ON, M8W 2W5, Canada

² Department of General Physics and Mathematics, Poltava V.G. Korolenko National Pedagogical University, 2 Ostrogradskogo str., Poltava 36003, Ukraine

³ Department of General Physics and Astronomy, Odesa I.I. Mechnikov National University, 2 Dvoryanskaya str., Odesa 65026, Ukraine

⁴ Family medicine center “Amedika”, LLC, 103B Semena Palia str., Odesa 65123, Ukraine

* **Correspondence:** Email: khorolskiy.alexey@gmail.com.

Abstract: We are devoted to the physical analysis of the habitat area of warm-blooded organisms – humans and many mammals. For this purpose, the establishment of equilibrium distribution of carbon dioxide in aqueous solutions of salts in contact with atmospheric air starting from some time is investigated. More precisely, the relaxation time of carbon dioxide, as a function of temperature and pH, is investigated. It is found that the pH-relaxation time τ_s is a very nontrivial function of temperature, pH values, and NaCl salt concentration. It was assumed that the minimum value of pH relaxation time corresponds to the optimal rate of physical processes in living matter. Using this selection principle and our experimental data, we have shown that the optimal temperature for human and mammalian life activity is close to $T_o \approx 37$ °C. The lower and upper temperature limits for their possible activity are close to $T_l \approx 30$ °C and $T_u \approx 42$ °C, respectively. The optimal value of pH_o , determined by the same selection principle, also becomes true if supplemented by the influence of albumin and other proteins.

Keywords: aqueous solutions; sodium chloride; carbon dioxide; pH; relaxation time; characteristic temperatures

1. Introduction

Why is this question formulated and within what framework will we attempt to answer it? Here, we will proceed with the basic assumption that modern life evolved from primitive forms that appeared in the primary ocean (see [1]). We take into account that the basic parameters of vital functions for humans and mammals are reduced to the lower and upper temperature, limiting their fields of activity, the optimum temperature of vital functions, as well as the permissible values of pH [2–5]. It should be noted here that temperature is a characteristic of a general type, while pH is a more subtle characteristic reflecting the more essential features of living matter [6–10]. We suggest that these parameters of life activity are determined by the most characteristic properties of water-salt solutions, i.e., the primary life forms were adapted to the primary solution in the ocean and did not change significantly during subsequent evolution. Our attempt is not a single one (see [11–14]). The main shortcoming of our attempts is the usage of indirect methods, such as the behavior of the shear viscosity [11], the temperature dependence of the heat capacity [12], the peculiarities of the mean-square displacement for biomolecules [11,14] and so on.

To achieve our goal, we study the temporal evolution of the pH for aqueous salt solutions in contact with atmospheric gases, including carbon dioxide, as a function of temperature and concentration for the salt NaCl. The main focus is to determine the characteristic time $\tau_S(T, pH)$, during which the equilibrium value of pH is established in the solution after its preparation. Similar processes take place in the blood plasma during the transport of oxygen and carbon dioxide.

In this regard, we assume that the optimal value of $\tau_S(T, pH)$ is defined as the minimum value for $\tau_S(T, pH)$, considered as a function of temperature and the irreducible pH part. We will consider the values of T_o and pH_o corresponding to this optimum as parameters of optimal life activity. The values of temperatures T_l and T_u limiting the vitality interval will be regarded as those within which $\tau_S(T, pH)$ has a fine structure. Here, the fine structure of $\tau_S(T, pH)$ is related to the influence of salts, as the electric fields of cations and anions stimulate changes in pH and $\tau_S(T, pH)$ (see [15]).

Accordingly, in this paper, we plan to: 1) present the results of $\tau_S(T, pH)$ as a function of temperature and salt concentration; 2) construct $\tau_S(T, pH)$ as a function of temperature and pH; 3) determine the optimal values of T_o and pH_o leading to the minimum value of τ_S ; 4) discuss the results obtained and the relationship to those observed for humans and mammals. The importance of the similarity law for curves corresponding to different salts concentrations is discussed separately.

2. Materials and methods

Freshly prepared distilled water of purity class 2 (according to ISO 3696 standard [16]) obtained from the Adrona Crystal EX Double Flow water purification system (Adrona SIA, Latvia) was used. A 0.9 wt.% aqueous sodium chloride solution (saline) for infusions of pharmaceutical quality (Darnitsa, Ukraine) was used as an initial solution. Solutions were prepared gravimetrically using Radwag AS 220.R2 scales (Radwag, Poland) with an error of ± 0.1 mg. Total relative error of mass measurement did not exceed 0.05 %. Ultrathermostat UTU-10 (Krakow, Poland) with error ± 0.1 K was used as a thermostat. For the salt concentration, we use the value ζ determined by the number of water molecules N_w per one salt ion N_S , i.e.:

$$\zeta = N_w / N_s . \quad (1)$$

Experimental pH measurements were performed in the temperature range (294 – 323) K for solutions with sodium chloride concentration $\zeta = (180, 215, 270, 360, 540, 675, 900, 1620)$.

pH was measured according to IUPAC recommendations [17,18] using an AZ Bench Top Water Quality Meter 86505 (AZ Instrument Corp., Taiwan) with a thermosensitive probe. The total relative error of the pH measurement was determined to be 0.5 % [19,20]. Before measurements, the pH meter was calibrated with standard buffer solutions with pH 4.00 and pH 7.00 at 25.0 °C.

To measure the time dependence of pH, 30 cm³ solutions were prepared at room temperature and stirred with a magnetic stirrer. Then, the solutions were placed in identical measuring vessels, and the samples were placed in a thermostat for 30 minutes until the first (zero time) measurement, when the solution was in contact with atmospheric air. The contact of aqueous sodium chloride solution with atmospheric carbon dioxide occurred through the free surface of the solution, which was the same in all measurements and was 8.14 cm².

We then analyze the sources of errors in measuring the pH. It was shown in [19] that the absolute error of pH measurements using a pH meter with two-point calibration (with automatic temperature compensation and a combined glass electrode) cannot be better than ± 0.02 units of pH. The main problem in calculating the error of instrumental pH measurements is the residual liquid transition potential, as well as the following causes: asymmetry potential, mixing effects, memory effects, temperature effects (e.g., temperature gradients over the electrode), membrane clogging, electrical noise (cable shielding), cross-contamination and carbonate exchange (in alkaline calibration buffers) [19,20]. In [21], it is shown that taking into account all the above uncertainty factors when measuring the pH in water and dilute aqueous solutions in the pH range (3.5–7.5) leads to the value of the absolute error of measurement $\pm (0.10\text{--}0.14)$ pH units. It was shown in [22] that the purity of the used reagents and knowledge of the exact concentration of the solutions have a significant influence on the pH determination of a solution by means of instrumental measurements. The latter cause accounts for 30% of the relative error in measuring the pH of an aqueous NaCl solution [22].

It should be emphasized that pH measurements of high-purity water are usually unstable and can be inaccurate due to its low ionic strength and low buffer capacity [23]. In other words, difficulties in pH measuring are due to the high resistivity of the solution and the unstable operation of the pH meter measuring electrodes [16,24]. The pH of freshly produced high-purity water can range from pH 5.0 to 8.0 and decrease rapidly after dispensing from the water treatment system. Therefore, pH is not considered an indicator of high-purity water quality [16]. Nevertheless, this circumstance does not contradict the purpose of the study, because we are not interested in the exact pH values of the solutions, but in the trend of the pH of the solutions over time.

3. Time evolution of the pH of aqueous sodium chloride solutions

Our experiments were performed at the natural pressure of atmospheric air. Nevertheless, we briefly discuss the experiments with the controlled gas composition. In works [25,26], it was shown that, in aqueous NaCl solutions saturated with carbon dioxide, pH value decreases with the growth of the NaCl concentration, provided that the temperature and the partial pressure of carbon dioxide remain constant. In work [27], a decrease of pH was observed in aqueous NaCl solutions saturated with carbon

dioxide, when the temperature grew, but the salt concentration remained constant. However, theoretical calculations in works [28,29] predicted a slight reduction of pH in aqueous NaCl solutions saturated with carbon dioxide: by approximately 0.01 pH unit as compared with pure water. As a result, a confusion, as if the addition of salt has almost no effect on the pH value. The contradiction between the experimental data and the results of theoretical calculations requires more thorough systematic research.

The character of the temporal evolution of the pH depending on the salt concentration, expressed in the number ζ of water molecules per cation (the corresponding molar concentration of salt is equal to $x_s = 1/(1+\zeta)$ [15]), is shown in Figure 1.

With satisfactory accuracy experimental data are fitted by the expression:

$$pH(t) = pH_{eq}(\zeta) + A(\zeta) \exp\left(-\frac{t}{\tau_s(\zeta)}\right). \quad (2)$$

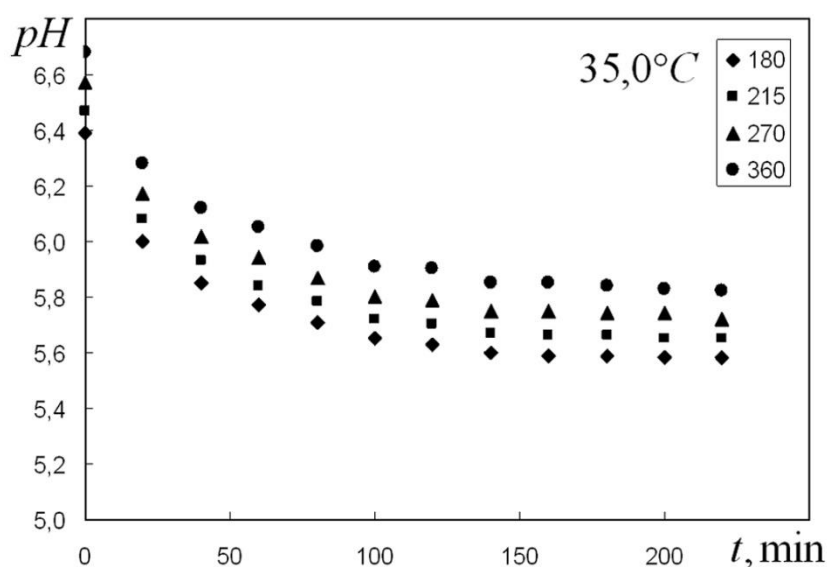


Figure 1. The temporal dependence of the pH at the temperature 35 °C for concentrations $\zeta = 180, 215, 270$ and 360.

The initial and equilibrium values of the pH are connected between by the relation:

$$pH(0) = pH_{eq}(T) + A(\zeta). \quad (3)$$

It is accepted that the equilibrium values of the pH depend only of the temperature according to:

$$pH_{eq}(t) = a - bT, \quad (4)$$

where the coefficients: $a = 5.97$, $b = 0.015$, correspond to those presented in paper [15], T is temperature in degrees Celsius.

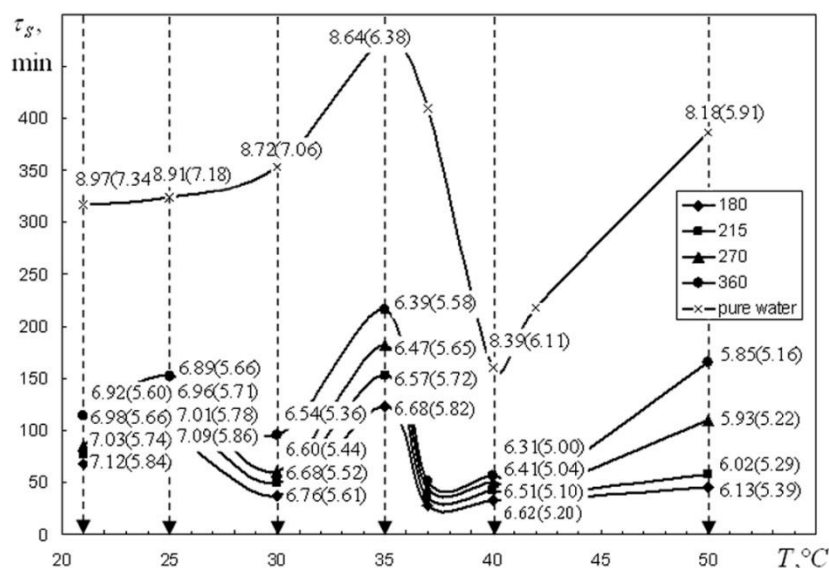


Figure 2. Temperature dependences of the relaxation time $\tau_s(T, \zeta)$ for different salt concentrations: $\zeta = (180, 215, 270, 360)$. The values of the pH in initial and final (equilibrium) positions (the last are taken in brackets) are given on isothermes near the intersection points.

3.1. Temperature dependence of $\tau_s(T, \zeta)$

In this subsection, we closely examine the temperature dependences of the relaxation time $\tau_s(T, \zeta)$ for different salt concentrations [15,30], and we also indicate the pH values at the points corresponding to the intersections of the sixth vertical lines (isotherms) with the curves $\tau_s(T, \zeta)$ (Figure 2).

Thus, the intersection point, determined by coordinates ($T = 35$ °C, $\zeta = 180$), corresponds to the relaxation curve, having the initial value $pH(0)$ 6.68 and the final one $pH(t_f)$ 5.82. The values of pH on isothermes are in fact the irreducible parts of pH that do not reduce due to temperature.

We will now discuss the basic properties of the temperature dependences for $\tau_s(T, \zeta)$: 1) $\tau_s(T, \zeta)$ -profile for pure water is characterized by the strongest changes in the relaxation time from the monotonic temperature dependence. It seems natural that $\tau_s(T, \zeta)$ should decrease with temperature. As can be seen, the most significant deviation from the monotonic behavior is observed in the interval ((30÷45) °C); 2) an addition of NaCl salt in amounts close to the human blood plasma ($\zeta = (180, 215, 270, 360)$) leads to the appearance of the fine structure: 1) the left oscillation is formed in the interval: (20÷35) °C and 2) the right, more asymmetric, is formed in the interval: (35 ÷ 42) °C. The minimum values of $\tau_s(T, \zeta)$ are observed at $T_l = 30$ °C, referring to the left oscillation, and at $T_o = 37$ °C and $T_u = 42$ °C, referring to the right oscillation. It is immediately suggested here that 1) (T_l, T_u) form the limit temperatures for the human and many mammalian life interval and 2) T_o is the optimum temperature for human and many mammalian life intervals. These results will be discussed further in the next subsection; 3) on each isotherm, the value of $\tau_s(T, \zeta)$ is a non-monotonic function of $pH(\zeta)$. To explain this effect, it should be taken into account that the dissociation energy for water molecules surrounding cations is markedly less compared to the energy characteristic of pure water.

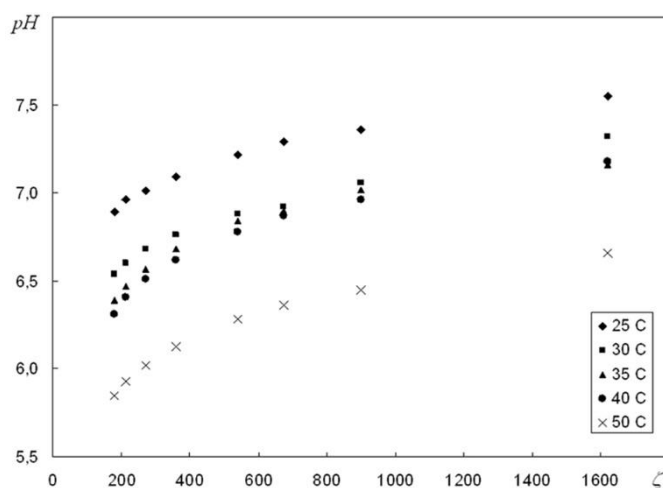


Figure 3. pH as a function of the salt concentration at several temperatures.

The corresponding effect for anions is noticeably smaller because the radii of the cations are smaller.

3.2. Reducible and irreducible parts of the pH

The pH values for $\zeta = 1620$ are actually the same as in pure water. Thus, the difference:

$$pH_{irr}(T, \zeta) = pH(T, \zeta) - pH(T, \zeta = 1620), \quad (5)$$

allows us to isolate the irreducible part $pH_{irr}(T, \zeta)$ of the pH at each isotherm. A decrease in ζ leads to an increase in the hydrogen density, i.e., an increase in $|pH_{irr}(T, \zeta)|$. In order of magnitude $|pH_{irr}(T, \zeta)| \sim 1$. The behavior of $pH_{irr}(T, \zeta)$ versus concentration ζ is presented in Figure 4.

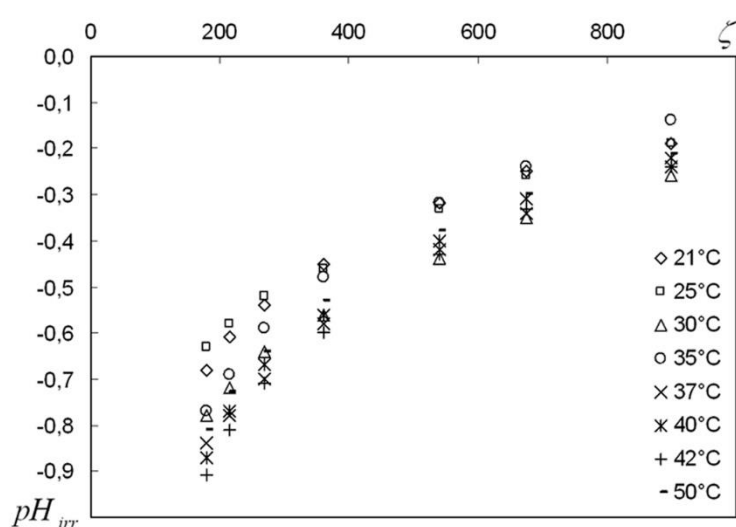


Figure 4. The irreducible part $pH_{irr}(T, \zeta)$ for aqueous NaCl solutions as a function of concentration at several temperatures.

Considering $pH(T, \zeta)$ as a superposition:

$$pH(T, \zeta) = pH_{red}(T, \zeta) + pH_{irr}(T, \zeta), \quad (6)$$

for the concentration dependence of $pH_{red}(T, \zeta)$ at the same temperatures we obtain (Figure 5):

$$pH_{red}(T, \zeta) = pH(T, \zeta) - pH_{irr}(T, \zeta). \quad (7)$$

The temperature dependences of $pH_{red}(T, \zeta)$ and $pH_{irr}(T, \zeta)$ at fixed concentrations are more informative in many relations (Figure 6). Here, we want to focus our attention on the interconnection of $pH_{irr}(T, \zeta)$ with physiological peculiarities of the life activity of human and mammals.

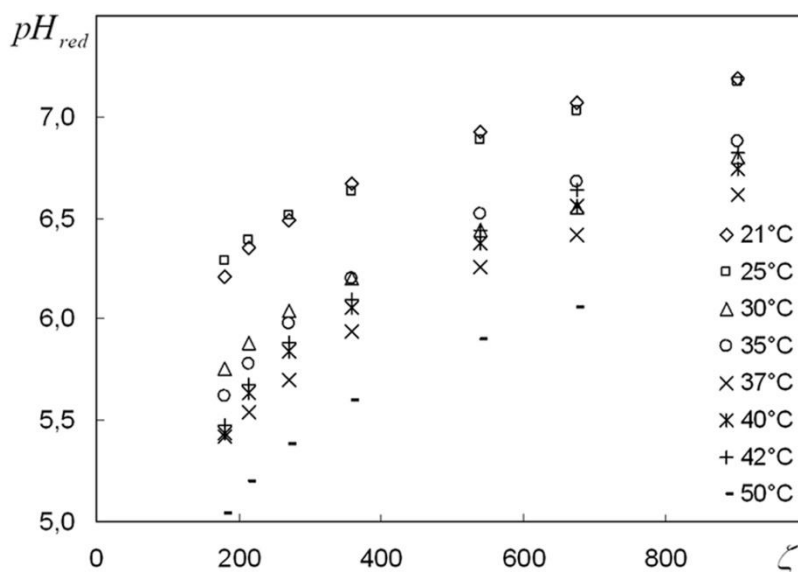


Figure 5. The concentration dependency of $pH_{red}(T, \zeta)$ for aqueous NaCl solutions at corresponding temperatures.

As we see from our analysis: 1) the temperatures dependences of $pH_{red}(T, \zeta)$ are close to rectilinear ones similarly to that as it has a place for pure water. It testifies about their similar physical nature, generated by binary high-energetic collisions [15]; 2) the temperature dependences of $pH_{irr}(T, \zeta)$ are more complicated, they disintegrate in two series: a) $180 < \zeta < \zeta_*$, $\zeta_* \approx 300$ and b) $\zeta_* < \zeta < 900$ having different structure of curves. The minimal values of $pH_{irr}(T, \zeta)$ curves from the first series are observed near $T_u \approx 42^\circ\text{C}$, which according to [12,14,30] can be interpreted as the upper limit for temperatures of the life activity for human and mammals.

It is verified, that the values of $pH_{irr}(T, \zeta)$ averaged on temperature, satisfy the equation:

$$\langle pH_{irr}(T, \zeta) \rangle_T \approx \zeta_1 / \zeta + \zeta_2 / \zeta^2 + \dots, \quad \zeta_1 \approx 178, \quad \zeta_2 \approx 4417, \dots \quad (8)$$

that leads to the asymptotic behavior: $pH_{irr}(T, \zeta) \rightarrow 0$ at $\zeta \rightarrow \infty$. These facts support our conclusion about different physical nature of $pH_{red}(T, \zeta)$ and $pH_{irr}(T, \zeta)$.

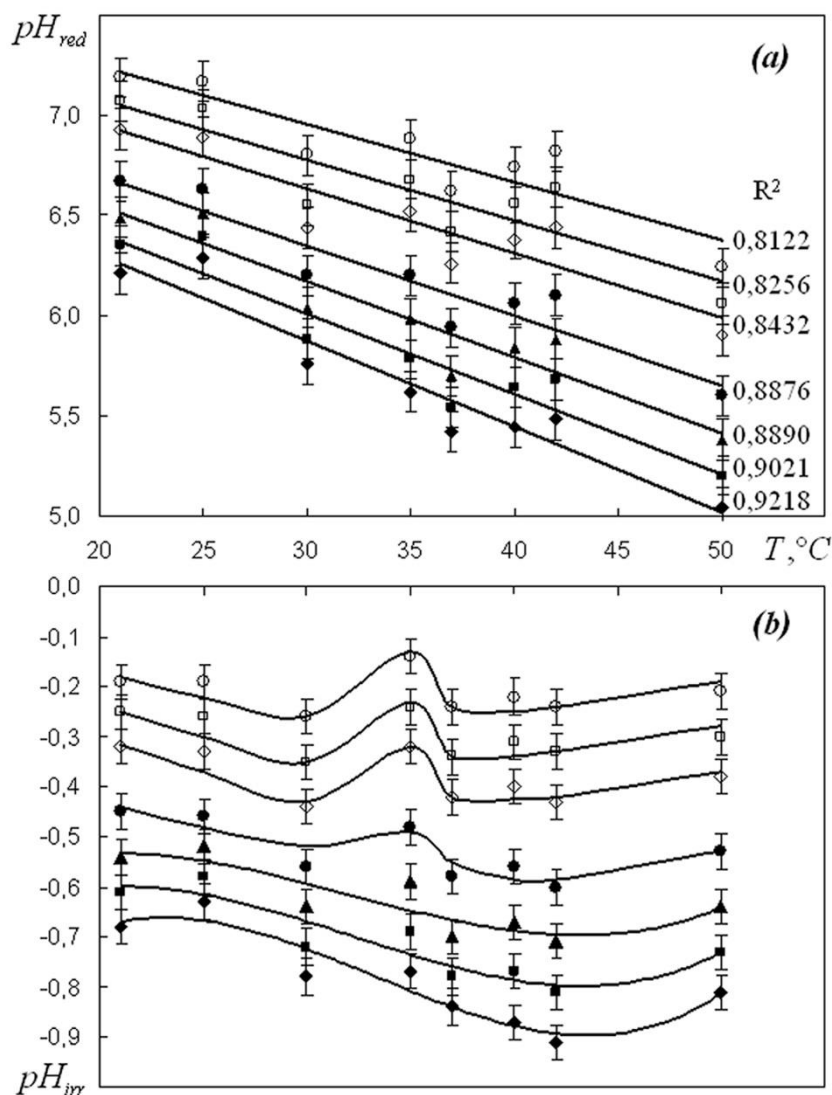


Figure 6. Temperatures dependency of $pH_{red}(T, \zeta)$ (a) and $pH_{irr}(T, \zeta)$ (b) for aqueous NaCl solutions at the following concentration of salt: $\zeta = 180$ (\blacklozenge), 215 (\blacksquare), 270 (\blacktriangle), 360 (\bullet), 540 (\diamond), 675 (\square), 900 (\circ). The degrees of fitting R^2 by linear functions are given in Figure 6(a).

3.3. Dependence of τ_s on pH

The relaxation times considered as functions of pH are shown in Figure 7. All curves have similar behavior, with rather sharp maxima, offset relative to each other, and asymmetrical details on them. The absolute minimum is observed at point $\zeta = 180$, pH 6.35, and it connects with the corresponding maximum and takes the value $\tau_s(pH) \approx 25$ min at point $T_o = 37$ $^{\circ}C$. The minimum value of τ_s on the same curve as $\zeta = 180$, but to the right of the maximum, is observed at $T_l \approx 32$ $^{\circ}C$. If the temperature becomes greater than $T_o = 37$ $^{\circ}C$, the relaxation time increases smoothly. On the contrary, if the temperature decreases relative to the optimum, the relaxation time increases. This means that to the left and to the right of the optimum point the behavior of living organisms is markedly different.

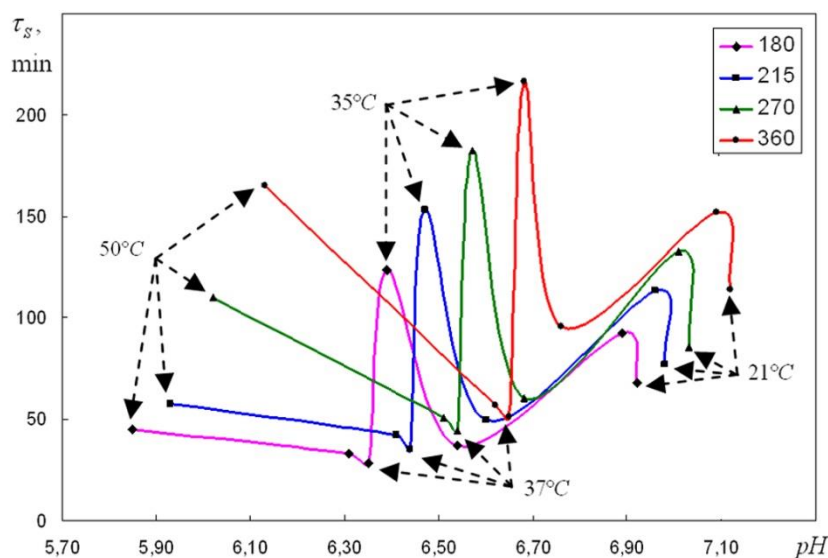


Figure 7. The relaxation time τ_s versus pH.

It is very important to note here that the minimum value of the relaxation time for carbon monoxide corresponds to the maximum rate of physiological processes in living matter. This fact is directly proved in [31], where the transport of oxygen by human blood is studied.

3.4. The principle of selection of optimal physiological states

We have established the existence of a close relationship between the characteristic points for the relaxation time $\tau_s(T, pH)$ in water-salt solutions and important physiological parameters of humans and mammals. This fact gives us grounds to formulate the principle of selection of optimal physiological states: the rate of transport processes in blood vessels should correspond to the minimum value of relaxation time for non-equilibrium states generated by oxygen and carbonic acid subsystems and considered as functions of temperature and pH.

Our major results were obtained when analyzing the relaxation time associated with the uptake of atmospheric gases, including carbon dioxide, i.e., the latter is an indicator of important physiological processes. From this point of view, it is very important to interpret the maxima observed in Figure 2 and Figure 4. The maximum observed at point $(T = 35\text{ }^\circ\text{C}, \zeta = 180)$ in Figure 2 indicates that even a small deviation from the optimal temperature $T_o \approx 37\text{ }^\circ\text{C}$ leads to a significant change in the rate of physiological processes. Furthermore, the maximum at $(T = 40\text{ }^\circ\text{C}, \zeta = 180)$ is relatively small, and therefore such a state for living matter is not categorically forbidden. There are animals and birds with $T_u \approx (45 \div 47)\text{ }^\circ\text{C}$ [32,33].

It is desirable to complement the analysis of the relaxation time for carbon dioxide adoption with other methods that allow a better understanding of the specifics of characteristic temperatures and pH values. For example, a study of incoherent neutron scattering in water [34–36] shows that the character of thermal motion in water changes radically at $T_u \approx 42\text{ }^\circ\text{C}$. The crystal-like character of thermal motion inherent in water for $T < T_u$ changes to argon-like for higher temperatures [11,13,14,37,38]. Such a conclusion can also be drawn from considering of the dipole relaxation time [39,40]. With good accuracy, the corresponding relaxation process changes its character at $T_d \approx T_u$. Extreme properties of

oxygen transport in blood vessels are discussed in detail in [31].

4. The demonstration of the similarity principle in the behavior of the relaxation time depending on the salt concentration

It follows from Figure 2 that the different curves resemble each other. This circumstance becomes more natural if we go to the dimensionless relaxation time of the type:

$$\tilde{\tau}(T, \zeta) = \frac{\tau_s(T, \zeta)}{\tau'_w(T, \zeta)}, \quad \tau'_w(T, \zeta) = \frac{\zeta}{\zeta_0} \tau_w(T), \quad \zeta_0 \approx 928, \quad (9)$$

where $\tau_w(T) = \lim_{\zeta \rightarrow \infty} \tau_s(T, \zeta)$ is the relaxation time for pure water. Formula (9), as follows from Figure 8, is particularly good for $\zeta = (180, 215, 270, 360)$ and $30^\circ\text{C} < T < 42^\circ\text{C}$.

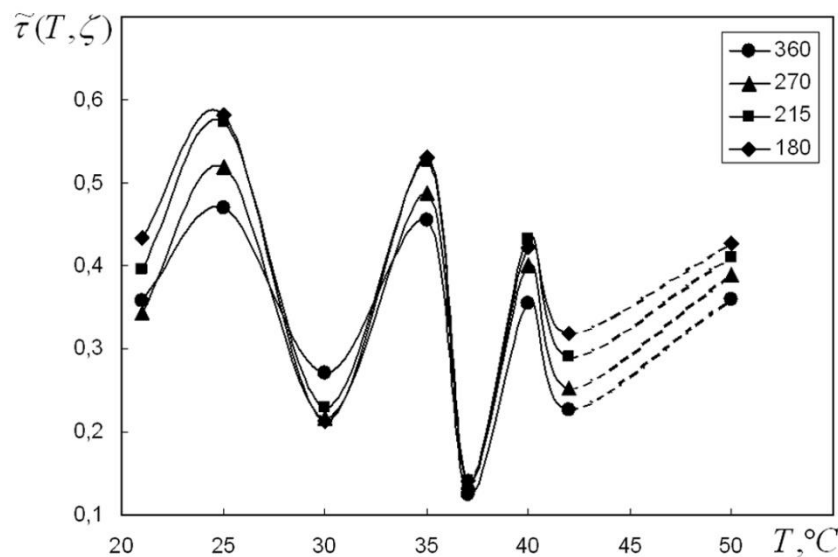


Figure 8. The dimensionless relaxation time $\tilde{\tau}(T, \zeta)$ as a function of temperature for $\zeta = (180, 215, 270, 360)$.

Rewriting (9) in the form:

$$\tau_s(T, \zeta) = \frac{\zeta}{\zeta_0} \tau_w(T) \tilde{\tau}(T, \zeta) \Rightarrow \frac{x_0}{x} \tau_w(T) \tilde{\tau}(T, \zeta). \quad (10)$$

we see that the relaxation time is proportional to only one simple multiplier, which has no universal character.

5. Conclusions

To investigate the physical nature of parameters characteristic of living matter—optimal temperature and lower and upper temperatures for the life interval—we have considered the relaxation

time of the pH parameter in water-salt solutions in contact with atmospheric carbon dioxide.

1. We have shown that all characteristic temperatures correspond to the minimum value of the relaxation time considered as a function of temperature and pH.
2. The relaxation time is proportional to the product of two universal functions. The coefficient of proportionality ζ_0/ζ is inversely proportional to the molar concentration of the salt.
3. The values of characteristic temperatures: $T_l \approx 30$ °C, $T_o \approx 37$ °C and $T_u \approx 42$ °C for humans and many mammals agree well with experimental data. Close values of T_l , T_u and T_o were also obtained in [12,14], but using less direct reasoning. The pH values, in particular pH_0 6.35, are smaller than the pH_0 7.35 value characteristic of humans [41–43]. This deviation is due to the additional influence of albumin and other proteins in the blood [38]. In the present work, it is shown that pH is temperature dependent and pH 7.35 exactly at $T_o \approx 37$ °C.

Use of AI tools declaration

The authors declare they have not used Artificial Intelligence (AI) tools in the creation of this article.

Conflict of interest

The authors declare no conflict of interest.

Author contributions

All authors contributed to the study's conception and design. AIF, OVK, NPM and AAG carried out the investigations and analyzed the outcomes. OVK prepared samples and conducted the experiments. AIF, OVK, NPM and AAG wrote the manuscript. AIF, OVK, NPM and AAG corrected and edited the manuscript. All authors revised and accepted the final version of the manuscript.

References

1. Falkowski PG, Knoll AH (2007) *Evolution of Primary Producers in the Sea*, New York: Academic Press.
2. Ivanov KP (2006) The development of the concepts of homeothermy and thermoregulation. *J Therm Biol* 31: 24–29. <https://doi.org/10.1016/j.jtherbio.2005.12.005>
3. Silva JE (2006) Thermogenic mechanisms and their hormonal regulation. *Physiol Rev* 86: 435–464. <https://doi.org/10.1152/physrev.00009.2005>
4. Clarke A, Pörtner HO (2010) Temperature, metabolic power and the evolution of endothermy. *Biol Rev Camb Philos Soc* 85: 703–727. <https://doi.org/10.1111/j.1469-185X.2010.00122.x>
5. He X, Aizenberg M, Kuksenok O, et al. (2012) Synthetic homeostatic materials with chemo-mechano-chemical self-regulation. *Nature* 487: 214–218. <https://doi.org/10.1038/nature11223>
6. Goldbeter A (2021) *Biochemical Oscillations and Cellular Rhythms: the Molecular Bases of Periodic and Chaotic Behaviour*, Cambridge: Cambridge University Press.
7. Liu M, Yuan L, Zhu C, et al. (2022) Peptide-modulated pH rhythms. *Chem Phys Chem* 23: e202200103. <https://doi.org/10.1002/cphc.202200103>

8. Cao Y, Wang M, Yuan Y, et al. (2019) Arterial blood gas and acid-base balance in patients with pregnancy-induced hypertension syndrome. *Exp Ther Med* 17: 349–353. <https://doi.org/10.3892/etm.2018.6893>
9. Rajkumar P, Pluznick JL (2018) Acid-base regulation in the renal proximal tubules: using novel pH sensors to maintain homeostasis. *Am J Physiol Renal Physiol* 315: F1187–F1190. <https://doi.org/10.1152/ajprenal.00185.2018>
10. Rand PW, Austin WH, Lacombe E, et al. (1968) pH and blood viscosity. *J Appl Physiol* 25: 550–559. <https://doi.org/10.1152/jappl.1968.25.5.550>
11. Bulavin LA, Fisenko AI, Malomuzh NP (2008) Surprising properties of the kinematic shear viscosity of water. *Chem Phys Lett* 453: 183–187. <https://doi.org/10.1016/j.cplett.2008.01.028>
12. Bulavin LA, Fisenko AI, Malomuzh NP (2013) What water properties are responsible for the physiological temperature interval limits of warm-blooded organisms? *arXiv*: 1307.7295 [physics.chem-ph]. <https://doi.org/10.48550/arXiv.1307.7295>
13. Fisenko AI, Malomuzh NP (2008) Role of the H-bond network in the creation of life-giving properties of water. *Chem Phys* 345: 164–172. <https://doi.org/10.1016/j.chemphys.2007.08.013>
14. Fisenko AI, Malomuzh NP (2009) To what extent is water responsible for the maintenance of the life for warm-blooded organisms? *Int J Mol Sci* 10: 2383–2411. <https://doi.org/10.3390/ijms10052383>
15. Stoliaryk OD, Khorolskyi OV (2022) Influence of atmospheric carbon dioxide on the acid-base balance in aqueous sodium chloride solutions. *Ukr J Phys* 67: 515–526. <https://doi.org/10.15407/ujpe67.7.515>
16. ISO 3696 (1987) *Laboratory Water for Analytical Purpose – Specification and Test Methods*.
17. Bates RG (1964) *Determination of pH: Theory and Practice*, John Wiley and Sons.
18. Buck RP, Rondinini S, Covington AK, et al. (2002) Measurement of pH. Definition, standards, and procedures (IUPAC Recommendations 2002). *Pure Appl Chem* 74: 2169–2200. <https://doi.org/10.1351/pac200274112169>
19. Leito I, Strauss L, Koort E, et al. (2002) Estimation of uncertainty in routine pH measurement. *Accredit Qual Assur* 7: 242–249. <https://doi.org/10.1007/s00769-002-0470-2>
20. Meinrath G, Spitzer P (2000) Uncertainties in determination of pH. *Mikrochim Acta* 135: 155–168. <https://doi.org/10.1007/s006040070005>
21. Kadis R, Leito I (2010) Evaluation of the residual liquid junction potential contribution to the uncertainty in pH measurement: A case study on low ionic strength natural waters. *Anal Chim Acta* 664: 129–135. <https://doi.org/10.1016/j.aca.2010.02.007>
22. Souza V, Ordine AP, Fraga ICS, et al. (2006) Effect of NaCl and HCl concentrations on primary pH measurement for the certification of standard materials. *Braz Arch Biol Technol* 49: 79–85. <https://doi.org/10.1590/S1516-89132006000200013>
23. Nora C, Mabic S, Darbouret D (2002) A theoretical approach to measuring pH and conductivity in high-purity water. *Ultrapure Water* 19: 56–61.
24. Melnik LA, Krysenko DA (2019) Ultrapure water: properties, production, and use. *J Water Chem Technol* 41: 143–150. <https://doi.org/10.3103/S1063455X19030020>
25. Hinds G, Cooling P, Wain A, et al. (2009) Technical note: Measurement of pH in concentrated brines. *Corrosion* 65: 635–638. <https://doi.org/10.5006/1.3319089>
26. Crolet JL, Bonis MR (1983) pH measurements in aqueous CO₂ solutions under high pressure and temperature. *Corrosion* 39: 39–46. <https://doi.org/10.5006/1.3580813>

27. Li X, Peng C, Crawshaw JP, et al. (2018) The pH of CO₂-saturated aqueous NaCl and NaHCO₃ solutions at temperatures between 308 K and 373 K at pressures up to 15 MPa. *Fluid Phase Equilib* 458: 253–263. <https://doi.org/10.1016/j.fluid.2017.11.023>
28. Story DA, Thistlethwaite P, Bellomo R (2000) The effect of PVC packaging on the acidity of 0.9% saline. *Anaesth Intens Care* 28: 287–292. <https://doi.org/10.1177/0310057x0002800306>
29. Reddi BA (2013) Why is saline so acidic (and does it really matter?) *Int J Med Sci* 10: 747–750. <https://doi.org/10.7150/ijms.5868>
30. Bulavin LA, Malomuzh NP, Khorolskyi OV (2022) Temperature and concentration dependences of pH in aqueous NaCl solutions with dissolved atmospheric CO₂. *Ukr J Phys* 67: 833–840. <https://doi.org/10.15407/ujpe67.7.833>
31. Guslisty AA, Malomuzh NP, Fisenko AI (2018) Optimal temperature for human life activity. *Ukr J Phys* 63: 809–815. <https://doi.org/10.15407/ujpe63.9.809>
32. Randall D, Burggren W, French K, et al. (1997) *Eckert animal physiology: Mechanisms and Adaptation*, 4 Eds., Freeman WH & Co.
33. Grigg GC, Beard LA, Augée ML (2004) The evolution of endothermy and its diversity in mammals and birds. *Physiol Biochem Zool* 77: 982–997. <https://doi.org/10.1086/425188>
34. Bulavin LA, Malomuzh NP, Pankratov KN (2006) Self-diffusion in water. *J Struct Chem* 4: S50–S60. <https://doi.org/10.1007/s10947-006-0377-6>
35. Bulavin LA, Lokotosh TV, Malomuzh NP (2008) Role of the collective self-diffusion in water and other liquids. *J Mol Liq* 137: 1–24. <https://doi.org/10.1016/j.molliq.2007.05.003>
36. Lokotosh TV, Malomuzh NP, Pankratov KN (2010) Thermal motion in water+ electrolyte solutions according to quasi-elastic incoherent neutron scattering data. *J Chem Eng Data* 55: 2021–2029. <https://doi.org/10.1021/je9009706>
37. Bulavin LA, Malomuzh NP (2006) Upper temperature limit for the existence of living matter. *J Mol Liq* 124: 136. <https://doi.org/10.1016/j.molliq.2005.11.027>
38. Bulavin LA, Gotsulskyi VY, Malomuzh NP, et al. (2020) Crucial role of water in the formation of basic properties of living matter. *Ukr J Phys* 65: 794–801. <https://doi.org/10.15407/ujpe65.9.794>
39. Okada K, Yao M, Hiejima Y, et al. (1999) Dielectric relaxation of water and heavy water in the whole fluid phase. *J Chem Phys* 110: 3026–3036. <https://doi.org/10.1063/1.477897>
40. Malomuzh NP, Makhlaichuk VN, Makhlaichuk PV, et al. (2013) Cluster structure of water in accordance with the data on dielectric permittivity and heat capacity. *J Struct Chem* 54: 205–220. <https://doi.org/10.1134/S0022476613080039>
41. Silverthorn DU (2018) *Human Physiology: An Integrated Approach*, 8 Eds., Pearson.
42. Hall JE, Hall ME (2020) *Guyton and Hall Textbook of Medical Physiology*, 14 Eds., Elsevier.
43. Bardic VYu, Fisenko AI, Magazù S, et al. (2020) The crucial role of water in the formation of the physiological temperature range for warm-blooded organisms. *J Mol Liq* 306: 112818. <https://doi.org/10.1016/j.molliq.2020.112818>



AIMS Press

© 2023 the Author(s), licensee AIMS Press. This is an open access article distributed under the terms of the Creative Commons Attribution License (<http://creativecommons.org/licenses/by/4.0>)